

An Autonomous Underwater Vehicle as an Underwater Glider and Its Depth Control

Moon G. Joo* and Zhihua Qu

Abstract: To provide a conventional autonomous underwater vehicle with gliding capability, we assume a moving battery and a buoyancy bag installed in a torpedo shaped autonomous underwater vehicle. We develop a mathematical model for the underwater vehicle and derive a stable gliding condition for it. Then an LQR controller is designed to control the zigzag depth of the vehicle, where the derived gliding condition is used as set-points of the control system. For control efforts in the gliding movement, the changes in the center of gravity and the net buoyancy are used, but neither thruster nor rudders are used. By using the gliding capability, the underwater vehicle can move to a farther location silently with less energy consumption and then start operating as a normal autonomous underwater vehicle. We show the feasibility of the proposed method by simulations using Matlab/Simulink.

Keywords: Autonomous underwater vehicle, depth control, LQR controller, underwater glider.

1. INTRODUCTION

Unmanned underwater vehicles have been developed in many countries. They can be roughly categorized into autonomous underwater vehicle (AUV) [1-4] and remotely operated vehicle (ROV) depending on the existence of tether that determines the autonomy level. AUV has on-board power and an on-board navigation system free from a tether, whereas ROV needs a tether to be supplied with power and steering control from the mother ship on the surface. A kind of hybrid AUV has also been developed which has the appearance of a conventional ROV having several thrusters to move to any direction but having no tether to transport power and control signals from the mother ship [5].

The conventional AUV has a torpedo shape. It has at least one thruster to go forward and rudders to change direction. The main area of application is military operation such as mine detection, terrain search, surveillance mission, and so on. Its advantages include a rapid response and a small turning radius. Since propeller thrust needs much energy, however, its operating time is limited to a few hours. On the other hand, the underwater glider (UWG) is a kind of AUV, which is shaped like a

winged airplane, and it performs a vertical zigzag movement to go forward by changing net buoyancy and the position of center of gravity [6-10]. UWG has been developed as a moving device for measuring temperature, salinity, water currents, etc. Since a very small amount of energy is required to inflate/deflate buoyancy bag or to push/pull the position of the battery position to change the center of gravity, UWG has a long operation time that lasts over a month and thus offers a long range coverage wider than 1000 km. However, it has disadvantages from the large turning radius which makes it difficult for precise position control.

Combining the good aspects of the conventional AUV and UWG is so natural that some of the combined underwater vehicles have been developed including an UWG without wings [11-13], an UWG with thruster and rudders [14], and an AUV with buoyancy bag and moving mass [15]. It can be another type of hybrid AUV in a sense that it can be used either as an AUV or as an UWG when necessary.

From the viewpoint of modeling for control purpose, a REMUS as a conventional AUV has been modeled in [1], where the AUV was assumed to be a rigid body and the external forces were mathematically obtained by the mechanical shapes of the hull, rudder, and sterns. Then the higher order terms of the external forces were ignored for simplification. Control inputs are the thruster velocity and the angle of sterns and rudders. There have been many control schemes reported such as PID, state feedback, sliding mode controller, neuro-fuzzy system, and so on [16-20]. The modeling for UWG was also conducted in [21,22] assuming the vehicle as a multi body system consisting of moving masses, a hull, and a variable mass buoyancy. External forces are not modeled directly, but obtained by the experiment or computational fluid dynamics software. They are described as functions of lift and drag depending on the angle of attack. Control inputs are the position of moving

Manuscript received June 23, 2014; revised September 26, 2014; accepted November 1, 2014. Recommended by Associate Editor Sung Jin Yoo under the direction of Editor Hyook Ryeol Choi.

This work was supported by Basic Science Research Program through the National Research Foundation of Korea(NRF) funded by the Ministry of Education, Science and Technology (2013 R1A1A4A01005930).

Moon G. Joo is with the Department of Information and Communications Engineering, Pukyong National University, Busan 608-737, Korea (e-mail: gabi@pknu.ac.kr).

Zhihua Qu is with the Department of Electrical Engineering and Computer Science, University of Central Florida, FL 32816, USA (e-mail: qu@ucf.edu).

mass and the mass of buoyancy. Some control schemes have been also reported [23-27]. In modeling of the hybrid AUV combining AUV and UWG, no unified modeling to handle both aspects of AUV and UWG has been reported yet to the best of our knowledge.

We, thus, propose a method of developing a unified model in order to add a gliding capability to the conventional AUV with which it can travel a long distance to a far location as an UWG and then operate as a normal AUV. The REMUS model in [1] is applied basically to use the already developed AUV control scheme in the AUV mode, and the work in [21] is adopted to derive the stable gliding condition in glider mode. This kind of hybrid AUV is advantageous from the aspect of quietness and energy saving under low current since it makes neither the noise nor the turbulence which an AUV inevitably makes because of the propeller thruster.

Section 2 develops a dynamic model for an AUV as an UWG. Section 3 derives the desired value of several necessary state variables for a stable gliding. Section 4 develops a linearized depth model to design a controller for vertical plane movement. Section 5 gives the simulation results using Matlab. A brief summary is followed in Section 6.

2. MODELING OF AUV AS UWG

Because the controllers of AUV such as REMUS have been widely studied, this paper focuses on controlling an AUV as UWG under the assumption that the AUV has a buoyancy bag and a moving battery pack in its hull as shown in Fig. 1. The purpose of modification is to endow the AUV with gliding capability which does not use any propeller propulsion.

It is worth to mention that unwinged UWGs in [11-13] are supposed to be operated as underwater gliders only. UWG in [14] focused on the change of parameter values due to the thruster and rudders from only the viewpoint of underwater glider. AUV in [15] is most similar and has a buoyancy bag and a moving battery in its hull, but it uses the buoyancy bag and the moving battery to achieve zero angle of attack at neutral buoyancy, for efficient propeller propulsion to minimize drag effect and thus to lengthen the operational time and range. In other words, the AUV operates always as a propeller-driven AUV, even though the vertical zigzag trajectory is used during its operation.

It is well known that an underwater robot with 6 degrees of freedom is described by nonlinear differential

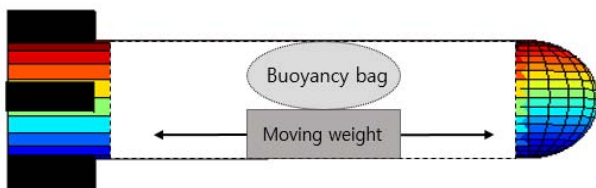


Fig. 1. AUV model with a moving mass and a buoyancy bag.

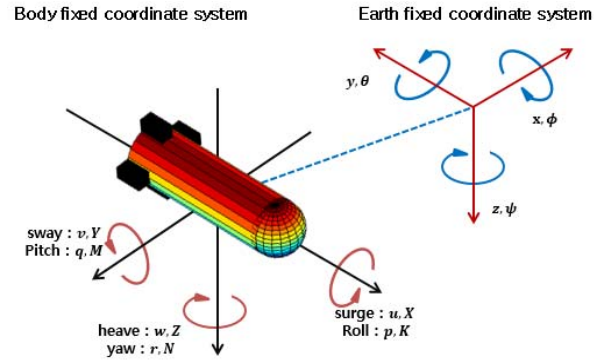


Fig. 2. State variables represented in the body fixed coordinate system and the earth fixed coordinate system.

equations using 12 state variables, $(x, y, z, u, v, w, \phi, \theta, \psi, p, q, r)$ as shown in Fig. 2 [28,29]. The NED coordinate is used as the earth fixed coordinate system.

Generally, the center of buoyancy is used as the origin of the body fixed coordinate, i.e., $x_b = y_b = z_b = 0$. The center of gravity in each direction is denoted as (x_g, y_g, z_g) . The mass of the vehicle is $m_v = m_h + \bar{m} + m_b$ where m_h is the mass of hull and its static components, \bar{m} is the moving mass such as battery pack, and m_b is the point mass buoyancy. The mass of the water displaced by the vehicle is denoted as m . Then the net buoyancy mass is $m_o = m_v - m$.

Now we have the following 12 dynamic equations. I_{xx} , I_{yy} and I_{zz} are moments of inertia in the body fixed coordinate. Among them, equations (1)-(6) are labeled to depict the vertical plane movement of the robot for later use.

$$m_v[\dot{u} - vr + wq - x_g(q^2 + r^2) + y_g(pq - \dot{r}) + z_g(pr + \dot{q})] = \sum X_{ext}, \quad (1)$$

$$m_v[\dot{v} - wp + ur - y_g(r^2 + p^2) + z_g(qr - \dot{p}) + x_g(qp + \dot{r})] = \sum Y_{ext}, \quad (2)$$

$$I_{xx}\dot{p} + (I_{zz} - I_{yy})qr + m_v[y_g(\dot{w} - uq + vp) - z_g(\dot{v} - wp + ur)] = \sum K_{ext},$$

$$I_{yy}\dot{q} + (I_{xx} - I_{zz})rp + m_v[z_g(\dot{u} - vr + wq) - x_g(\dot{w} - uq + vp)] = \sum M_{ext}, \quad (3)$$

$$I_{zz}\dot{r} + (I_{yy} - I_{xx})pq + m_v[x_g(\dot{v} - wp + ur) - y_g(\dot{u} - vr + wq)] = \sum N_{ext},$$

$$\dot{x} = u \cos \psi \cos \theta + v(\cos \psi \sin \theta \sin \phi - \sin \psi \cos \phi) + w(\cos \psi \sin \theta \sin \phi + \sin \psi \sin \phi), \quad (4)$$

$$\dot{y} = u \sin \psi \cos \theta + v(\sin \psi \sin \theta \sin \phi + \cos \psi \cos \phi) + w(\sin \psi \sin \theta \cos \phi - \cos \psi \sin \phi), \quad (5)$$

$$\dot{z} = -u \sin \theta + v \cos \theta \sin \phi + w \cos \theta \sin \phi,$$

$$\dot{\phi} = p + q \sin \phi \tan \theta + r \cos \phi \tan \theta,$$

$$\dot{\theta} = q \cos \phi - r \sin \phi, \quad (6)$$

$$\dot{\psi} = (q \sin \phi + r \cos \phi) / \cos \theta.$$

External forces exerted on the AUV [1] are written as

$$\begin{aligned}
\sum X_{ext} &= X_{HS} && ; \text{Hydro Static} \\
&+ X_{\dot{u}}\dot{u} + Z_{\dot{w}}w\dot{q} + Z_{\dot{q}}q\dot{q} \\
&- Y_{\dot{v}}v\dot{r} - Y_{\dot{r}}r\dot{r} && ; \text{Added Mass, Coriolis} \\
&+ X_{u|u}|u| && ; \text{Axial Drag} \\
&+ X_{prop} && ; \text{Propeller Thrust,} \\
\sum Y_{ext} &= Y_{HS} && ; \text{Hydro Static} \\
&+ Y_{\dot{v}}\dot{v} + Y_{\dot{r}}\dot{r} + X_{\dot{u}}u\dot{r} \\
&- Z_{\dot{w}}w\dot{p} - Z_{\dot{q}}p\dot{q} && ; \text{Added Mass, Coriolis} \\
&+ Y_{v|v}|v| + Y_{r|r}|r| && ; \text{Crossflow Drag} \\
&+ Y_{uvl}uv && ; \text{Body Lift} \\
&+ Y_{uu\delta r}u^2\delta r + Y_{uwf}uw + Y_{urf}ur && ; \text{Fin Lift,} \\
\sum Z_{ext} &= Z_{HS} && ; \text{Hydro Static} \\
&+ Z_{\dot{w}}\dot{w} + Z_{\dot{q}}\dot{q} - X_{\dot{u}}u\dot{q} \\
&+ Y_{\dot{v}}v\dot{p} + Y_{\dot{r}}r\dot{p} && ; \text{Added Mass, Coriolis} \\
&+ Z_{w|w}|w| + Z_{q|q}|q| && ; \text{Crossflow Drag} \\
&+ Z_{uwl}uw && ; \text{Body Lift} \\
&+ Z_{uu\delta s}u^2\delta s + Z_{uwf}uw \\
&+ Z_{uqf}uq && ; \text{Fin Lift,} \\
\sum K_{ext} &= K_{HS} && ; \text{Hydro Static} \\
&+ K_{\dot{p}}\dot{p} && ; \text{Added Mass, Coriolis} \\
&+ K_{p|p}|p| && ; \text{Rolling Drag Moment} \\
&+ K_{prop} && ; \text{Propeller Torque,} \\
\sum M_{ext} &= M_{HS} && ; \text{Hydro Static} \\
&+ M_{\dot{w}}\dot{w} + M_{\dot{q}}\dot{q} \\
&- (Z_{\dot{w}} - X_{\dot{u}})uw - Y_{\dot{v}}v\dot{p} && ; \text{Added Mass, Coriolis} \\
&+ (K_{\dot{p}} - N_{\dot{r}})rp - Z_{\dot{q}}uq && ; \text{Added Mass, Coriolis} \\
&+ M_{w|w}|w| + M_{q|q}|q| && ; \text{Crossflow Drag} \\
&+ M_{uwl}uw && ; \text{Body Lift Moment} \\
&+ M_{uu\delta s}u^2\delta s + M_{uwf}uw \\
&+ M_{uqf}uq && ; \text{Fin Lift,} \\
\sum N_{ext} &= N_{HS} && ; \text{Hydro Static} \\
&+ N_{\dot{v}}\dot{v} + N_{\dot{r}}\dot{r} - (X_{\dot{u}} - Y_{\dot{v}})uv \\
&+ Z_{\dot{q}}wp && ; \text{Added Mass, Coriolis} \\
&- (K_{\dot{p}} - M_{\dot{q}})pq + Y_{\dot{r}}ur && ; \text{Added Mass, Coriolis} \\
&+ N_{v|v}|v| + N_{r|r}|r| && ; \text{Crossflow Drag} \\
&+ N_{uvl}uv && ; \text{Body Lift Moment} \\
&+ N_{uu\delta r}u^2\delta r + N_{uwf}uw \\
&+ N_{urf}ur && ; \text{Fin Lift,}
\end{aligned}$$

where X_{prop} , K_{prop} , δs , and δr are the propeller propulsion, the propeller torque, the stern angle, and the

rudder angle, respectively.

The hydrostatic force on the underwater vehicle assuming a moving mass shifting only forward and backward ($y_g = 0$, $z_g = Z_G(const.)$) becomes

$$\begin{aligned}
X_{HS} &= -(W - B)\sin\theta, \\
Y_{HS} &= (W - B)\cos\theta\sin\phi, \\
Z_{HS} &= (W - B)\cos\theta\cos\phi, \\
K_{HS} &= y_gW\cos\theta\cos\phi - z_gW\cos\theta\sin\phi \\
&= Z_GW\cos\theta\sin\phi, \\
M_{HS} &= -z_gW\sin\theta - x_gW\cos\theta\cos\phi \\
&= -Z_GW\sin\theta - x_gW\cos\theta\cos\phi, \\
N_{HS} &= x_gW\cos\theta\sin\phi + y_gW\sin\theta \\
&= x_gW\cos\theta\sin\phi,
\end{aligned}$$

where

$$\begin{aligned}
W &= (m_h + \bar{m} + m_b)g, \\
B &= mg.
\end{aligned}$$

g is the gravitational acceleration constant.

3. STABLE GLIDING CONDITION

To find the stable gliding condition of the underwater vehicle, we adopt the method in [21], and then newly derive the desired values of necessary variables in this section.

Under the stable gliding condition where the lateral movement does not occur, the following holds;

$$\begin{aligned}
\dot{u} = \dot{v} = \dot{w} = 0, \quad v = 0, \quad \dot{p} = \dot{q} = \dot{r} = p = q = r = 0, \\
\phi = \psi = 0.
\end{aligned}$$

We add the restriction of using neither propulsion nor torque by thruster. Rudder and stern are not used in the glider mode, either;

$$X_{prop} = K_{prop} = 0, \quad \delta_r = \delta_s = 0.$$

Then the underwater vehicle suffers no external forces, therefore, the following equations are true;

$$\sum X_{ext} = -(W - B)\sin\theta_d + X_{u|u}|u_d||u_d| = 0, \quad (7)$$

$$\sum Z_{ext} = (W - B)\cos\theta_d + Z_{w|w}|w_d||w_d| + Z_{uw}u_dw_d = 0, \quad (8)$$

$$\sum M_{ext} = -(Z_G\sin\theta_d + x_g\cos\theta_d)W + M_{w|w}|w_d||w_d| + M_{uw}u_dw_d = 0, \quad (9)$$

where

$$\begin{aligned}
Z_{uw} &= Z_{uwl} + Z_{uwf}, \\
M_{uw} &= M_{uwa} + M_{uwl} + M_{uwf}, \quad M_{uwa} = -(Z_{\dot{w}} - X_{\dot{u}}),
\end{aligned}$$

and θ_d , u_d , and w_d are desired pitch angle, desired surge, and the desired sway, respectively.

The desired trajectory of the vehicle is normally

defined by the moving speed of the vehicle, $V_d = \sqrt{u_d^2 + w_d^2}$, and the angle of flight, ξ_d . The desired angle of attack is denoted as α_d , and it will be obtained soon. Given ξ_d and α_d , we have the pitch angle of the robot as

$$\theta_d = \xi_d + \alpha_d. \quad (10)$$

Furthermore, if $\alpha_d \ll 1$, then

$$\alpha_d (\text{rad}) = \tan^{-1} \left(\frac{w_d}{u_d} \right) \approx \frac{w_d}{u_d}. \quad (11)$$

Using (10) and (11), equations (7)-(9) are rewritten as

$$(W - B) \sin(\xi_d + \alpha_d) = X_{u|u|} u_d^2, \quad (12)$$

$$(W - B) \cos(\xi_d + \alpha_d) = -Z_{w|w|} \alpha_d |\alpha_d| u_d^2 - Z_{uw} \alpha_d u_d^2, \quad (13)$$

$$x_g W \cos(\xi_d + \alpha_d) = -Z_G W \sin(\xi_d + \alpha_d) + M_{w|w|} \alpha_d |\alpha_d| u_d^2 + M_{uw} \alpha_d u_d^2. \quad (14)$$

Dividing (12) by (13) gives (15), from which we obtain α_d :

$$\tan(\xi_d + \alpha_d) = \frac{X_{u|u|}}{-Z_{w|w|} \alpha_d |\alpha_d| - Z_{uw} \alpha_d}. \quad (15)$$

Once α_d is determined, from (12) and (13), the desired mass of variable buoyancy for the given trajectory is calculated as

$$m_{bd} = m - m_h - \bar{m} \pm \frac{\sqrt{X_{u|u|}^2 + (Z_{w|w|} \alpha_d |\alpha_d| + Z_{uw} \alpha_d)^2}}{g} u_d^2. \quad (16)$$

Then, from (14), the desired center of mass for the trajectory is calculated as

$$x_{gd} = \frac{-Z_G (m_h + \bar{m} + m_{bd}) g \sin \theta_d + (M_{w|w|} \alpha_d |\alpha_d| + M_{uw} \alpha_d) u_d^2}{(m_h + \bar{m} + m_{bd}) g \cos \theta_d}. \quad (17)$$

With V_d and α_d , the desired surge and heave are calculated as

$$u_d = V_d \cos(\alpha_d), \quad w_d = V_d \sin(\alpha_d). \quad (18)$$

Table 1 shows the determined values for arbitrary chosen three flight angles when $X_{u|u|}/Z_{uw} = 0.1364$, $m = 32.314$. $Z_G = 0.02$ is assumed and that should be determined when an AUV is implemented. Note that ξ_d and V_d are the design parameters and they must be checked to give $\alpha_d \ll 1$ from (15).

4. DEPTH CONTROL OF THE VEHICLE

Because many successful trajectory control methods for the conventional AUV have been reported, we only consider the depth control regarding AUV as UWG.

Table 1. Desired values of parameters for stable gliding.

	downward			upward		
ξ_d (deg)	-30°	-45°	-60°	30°	45°	60°
α_d (deg)	12°	7°	4°	-12°	-7°	-4°
θ_d (deg)	-18°	-38°	-56°	18°	38°	56°
V_d (m/s)	0.30	0.30	0.30	0.30	0.30	0.30
u_d (m/s)	0.2936	0.2978	0.2993	0.2936	0.2978	0.2993
w_d (m/s)	0.0615	0.0364	0.0209	-0.0615	-0.0364	-0.0209
x_{gd} (m)	0.0080	0.0167	0.0305	-0.0080	-0.0167	-0.0305
Z_G (m)	0.02	0.02	0.02	0.02	0.02	0.02
m_{bd} (kg)	0.9436	0.8954	0.8778	0.7262	0.7743	0.7919

Along with the result of Section III, we design an LQR controller similar to the work in [21].

Setting $X_{prop} = 0$, $\delta s = 0$ and assuming

$$p = r = 0, \quad q = 0, \quad v = 0, \quad w = 0, \quad (19)$$

we rewrite the vertical plane equations (1)-(3) as

$$(m_v - X_{\dot{u}}) \dot{u} + m_v z_g \dot{q} = -(W - B) \sin \theta + (Z_{\dot{w}} - m_v) w q, \quad (20)$$

$$(m_v - Z_{\dot{w}}) \dot{w} - (m_v x_g + Z_{\dot{q}}) \dot{q} = (W - B) \cos \theta + (m_v + Z_{uq}) u q + Z_{uw} u w, \quad (21)$$

$$m_v z_g \dot{u} - (m_v x_g + M_{\dot{w}}) \dot{w} + (I_{yy} - M_{\dot{q}}) \dot{q} = -(Z_G \sin \theta + x_g \cos \theta) W + M_{uw} u w - m_v Z_G w q + (M_{uq} - m_v x_g) u q, \quad (22)$$

where

$$Z_{uw} = Z_{uwl} + Z_{uwf}, \quad Z_{uq} = Z_{uqa} + Z_{uqf}, \quad Z_{uqa} = -X_{\dot{u}},$$

$$M_{uw} = M_{uwa} + M_{uwl} + M_{uwf}, \quad M_{uwa} = -(Z_{\dot{w}} - X_{\dot{u}}),$$

$$M_{uq} = M_{uqa} + M_{uqf}, \quad M_{uqa} = -Z_{\dot{q}}.$$

To get a constant inverse matrix later shown, we set $m_v = m_h + \bar{m} + m_b \approx m_h + \bar{m} = m_{v0}$ in the left side of (20)-(22). Generally, it is true since $m_h + \bar{m} \gg m_b$. Letting an operating point $(u, w, \theta, q, x_g, m_b)_{op}$ as $(u_d, w_d, \theta_d, q_d, x_{gd}, m_{bd})$, we can linearized the right side of equations around the operating point as

$$(m_{v0} - X_{\dot{u}}) \dot{u} + m_{v0} z_g \dot{q} \approx X_{op} + (Z_{\dot{w}} - m_{vd}) w_d \Delta q - (W_d - B) \cos \theta_d \Delta \theta - g \sin \theta_d \Delta m_b, \quad (23)$$

$$(m_{v0} - Z_{\dot{w}}) \dot{w} - (m_{v0} x_g + Z_{\dot{q}}) \dot{q} \approx Z_{op} + Z_{uw} w_d \Delta u + Z_{uw} u_d \Delta w + (m_{vd} + Z_{uq}) u_d \Delta q - (W_d - B) \sin \theta_d \Delta \theta + g \cos \theta_d \Delta m_b, \quad (24)$$

$$m_{v0} z_g \dot{u} - (m_{v0} x_g + M_{\dot{w}}) \dot{w} + (I_{yy} - M_{\dot{q}}) \dot{q} \approx M_{op} + M_{uw} w_d \Delta u + M_{uw} u_d \Delta w - W \cos \theta_d \Delta x_g + (-m_{vd} Z_G w_d + (M_{uq} - m_{vd} x_{gd}) u_d) \Delta q + (-Z_G \cos \theta_d + x_{gd} \sin \theta_d) W \Delta \theta, \quad (25)$$

where

$$\begin{aligned}
\Delta u &= u - u_d, \quad \Delta w = w - w_d, \quad \Delta q = q - q_d, \\
\Delta \theta &= \theta - \theta_d, \quad \Delta x_g = x_g - x_{gd}, \quad \Delta m_b = m_b - m_{bd}, \\
m_{vd} &= m_h + \bar{m} + m_{bd}, \quad W_d = m_{vd} g, \\
X_{op} &= -(W_d - B) \sin \theta_d, \\
Z_{op} &= (W_d - B) \cos \theta_d + Z_{uw} u_d w_d, \\
M_{op} &= -(Z_G \sin \theta_d + x_{gd} \cos \theta_d) W_d + M_{uw} u_d w_d.
\end{aligned}$$

The actuator dynamics for the change in the center of gravity and the change in the mass of buoyancy bag are linearized as

$$\begin{aligned}
\dot{x}_g &= b_x u_x \approx x_{g,op} + b_x u_x, \\
\dot{m}_b &= b_m u_b \approx m_{b,op} + b_m u_b,
\end{aligned} \quad (26)$$

where

$$x_{g,op} = 0, \quad m_{b,op} = 0.$$

With (19), equations (4)-(5) representing the NED position of the robot in the vertical plane is written as

$$\begin{aligned}
\dot{x} &= u \cos \theta + w \sin \theta, \\
\dot{z} &= -u \sin \theta + w \cos \theta.
\end{aligned}$$

A coordinate transform (27) is required to control with ease the deviated distance between the desired trajectory and the vehicle;

$$\begin{bmatrix} x' \\ z' \end{bmatrix} = \begin{bmatrix} \cos \xi_d & -\sin \xi_d \\ \sin \xi_d & \cos \xi_d \end{bmatrix} \begin{bmatrix} x \\ z \end{bmatrix}. \quad (27)$$

The transformed variable z' means the perpendicular distance from the desired trajectory as shown in Fig. 3 and the purpose of the control is to make z' as 0. x' is not considered as a control purpose like as most of the UWG does not.

Differentiating (27), the z' part becomes

$$\begin{aligned}
\dot{z}' &= \sin \xi_d \dot{x} + \cos \xi_d \dot{z} \\
&= u(\sin \xi_d \cos \theta - \cos \xi_d \sin \theta) \\
&\quad + w(\sin \xi_d \sin \theta + \cos \xi_d \cos \theta) \\
&\approx z'_{op} - \sin \alpha_d \Delta u + \cos \alpha_d \Delta w \\
&\quad - (u_d \cos \alpha_d + w_d \sin \alpha_d) \Delta \theta,
\end{aligned} \quad (28)$$

where

$$z'_{op} = -u_d \sin \alpha_d + w_d \cos \alpha_d = 0 \quad (\because \tan \alpha_d = w_d / u_d).$$

With (19), the pitch equation (6) of the robot is

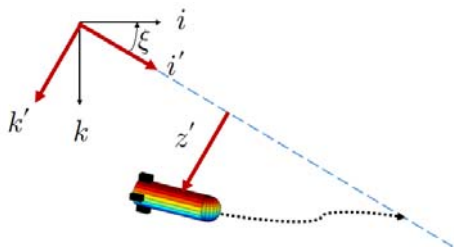


Fig. 3. Coordinate transform.

linearized as

$$\dot{\theta} = q \approx q_{op} + \delta q, \quad (29)$$

where

$$q_{op} = 0.$$

In summary, the matrix version of (23)-(26), (28), and (29) is written as

$$M \dot{X} = A \Delta X + B U + F, \quad Y = C \Delta X, \quad (30)$$

where

$$\Delta X = X - X_d, \quad X = [u \ w \ q \ z' \ \theta \ x_g \ m_b]^T,$$

$$X_d = [u_d \ w_d \ 0 \ 0 \ \theta_d \ x_{gd} \ m_{bd}]^T, \quad U = [u_x \ u_b]^T,$$

$M =$

$$\begin{bmatrix} m_{v0} - X_{\dot{u}} & 0 & m_{v0} Z_G & 0 & 0 & 0 & 0 \\ 0 & m_{v0} - Z_{\dot{w}} & -(m_{v0} x_g + Z_{\dot{q}}) & 0 & 0 & 0 & 0 \\ m_{v0} Z_G & -(m_{v0} x_g + M_{\dot{w}}) & I_{yy} - M_{\dot{q}} & 0 & 0 & 0 & 0 \\ 0 & 0 & 0 & 1 & 0 & 0 & 0 \\ 0 & 0 & 0 & 0 & 1 & 0 & 0 \\ 0 & 0 & 0 & 0 & 0 & 1 & 0 \\ 0 & 0 & 0 & 0 & 0 & 0 & 1 \end{bmatrix},$$

$$\begin{bmatrix} 0 & 0 & (Z_{\dot{w}} - m_{vd}) w_d & 0 \\ Z_{uw} w_d & Z_{uw} u_d & (m_{vd} + Z_{uq}) u_d & 0 \\ M_{uw} w_d & M_{uw} u_d & a_{33} & 0 \\ -\sin \alpha_d & \cos \alpha_d & 0 & 0 \\ 0 & 0 & 1 & 0 \\ 0 & 0 & 0 & 0 \\ 0 & 0 & 0 & 0 \\ -(W_d - B) \cos \theta_d & 0 & -g \sin \theta_d \\ -(W_d - B) \sin \theta_d & 0 & g \cos \theta_d \\ a_{35} & -W_d \cos \theta_d & 0 \\ a_{45} & 0 & 0 \\ 0 & 0 & 0 \\ 0 & 0 & 0 \\ 0 & 0 & 0 \end{bmatrix},$$

$$a_{33} = (M_{uq} - m_{vd} x_{gd}) u_d - m_{vd} Z_G w_d,$$

$$a_{35} = (-Z_G \cos \theta_d + x_{gd} \sin \theta_d) W_d,$$

$$a_{45} = -u_d \cos \alpha_d - w_d \sin \alpha_d,$$

$$\begin{bmatrix} 0 & 0 \\ 0 & 0 \\ 0 & 0 \\ 0 & 0 \\ 0 & 0 \\ b_x & 0 \\ 0 & b_m \end{bmatrix}, \quad F = \begin{bmatrix} X_{op} \\ Z_{op} \\ M_{op} \\ q_{op} \\ z'_{op} \\ x_{g,op} \\ m_{b,op} \end{bmatrix}, \quad C = \begin{bmatrix} 1 & 0 & 0 & 0 & 0 & 0 & 0 \\ 0 & 1 & 0 & 0 & 0 & 0 & 0 \\ 0 & 0 & 1 & 0 & 0 & 0 & 0 \\ 0 & 0 & 0 & 1 & 0 & 0 & 0 \\ 0 & 0 & 0 & 0 & 1 & 0 & 0 \end{bmatrix}.$$

Because M is a constant matrix, if it is invertible, the state equation (30) is rewritten as

$$\begin{aligned} \dot{X} &= M^{-1}A\Delta X + M^{-1}BU + M^{-1}F \\ &= \tilde{A}\Delta X + \tilde{B}U + \tilde{F}, \end{aligned}$$

where

$$\tilde{A} = M^{-1}A, \quad \tilde{B} = M^{-1}B, \quad \tilde{F} = M^{-1}F.$$

Introduce the desired state equation, we set;

$$\begin{aligned} \dot{X}_d &= \tilde{A}\Delta X_d + \tilde{B}U_d + \tilde{F}, \\ U_d &= [0 \quad 0]^T. \end{aligned}$$

Using the difference between above two matrix equations, we construct a regulator equation as follows and the control purpose is to make $\Delta X \rightarrow 0$;

$$\begin{aligned} \Delta \dot{X} &= \tilde{A}\Delta X + \tilde{B}\Delta U, \\ \Delta U &= U - U_d = U. \end{aligned}$$

Pole placement or LQR can be used to determine the control input:

$$\Delta U = U = -K\Delta X. \quad (31)$$

5. SIMULATION

To verify and evaluate the feasibility of the proposed method, simulations using Matlab/Simulink shown in Fig. 4 were performed, where the overall system was considered as a discrete control system using ZOH with 1 second sampling time as shown in Fig. 5.

In the simulation, the following reasonable measurement noises are added:

$$\begin{aligned} u_n, v_n, w_n &: rand(-0.0051, 0.0051) ; \pm 0.01 \text{ knot (DVL)}, \\ p_n, q_n, r_n &: rand(-0.2618, 0.2618) ; \pm 15^\circ / \text{sec (DVL)}, \\ x_n, y_n, z_n &: rand(-0.5000, 0.5000) ; \pm 0.5 \text{ m (GPS)}, \\ \phi_n, \theta_n, \varphi_n &: rand(-0.0175, 0.0175) ; \pm 1^\circ \text{ (IMU)}, \end{aligned}$$

where $(\cdot)_n$ denotes the noise to each variable, and $rand(\cdot)$ denotes a random value within the given range. The values are dictated from the specification of NavQuest 600 Micro by LinkQuest Inc. for DVL, AsteRx1 by Septentrio for GPS, and MTi by Xsens for IMU.

The change ratios in the buoyancy mass and the center of gravity are assumed as 1 Kg/min and 1 mm/sec, respectively; $b_x = 0.0167$, $b_m = 0.001$.

Table 2 lists the simulation parameters for AUV given in [1] except for the movable mass, that is arbitrarily chosen as $\bar{m} = 1$ kg.

To control the zigzag depth forcing the AUV go forward, an LQR controller with 1 second sampling time is designed using a built-in “dlqr” command in Matlab. The weighting factors are selected to give stress on depth, pitch, the center of gravity, and the buoyance mass and are shown as

Hybrid Autonomous Underwater Vehicle : AUV + Glider

At the end of the simulation, XY graph, XZ graph, depth graph, and XYZ graph appear. tested in Matlab R2012a. 2014.1 <http://cal.pnu.ac.kr>

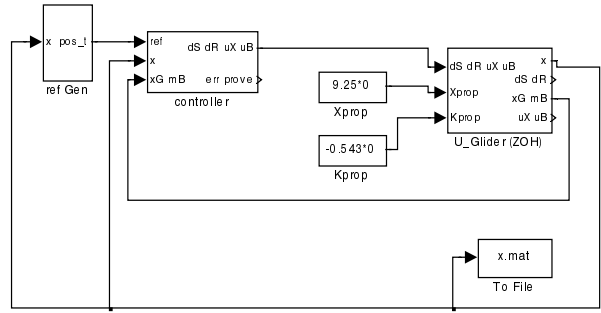


Fig. 4. Simulation using Matlab/simulink.

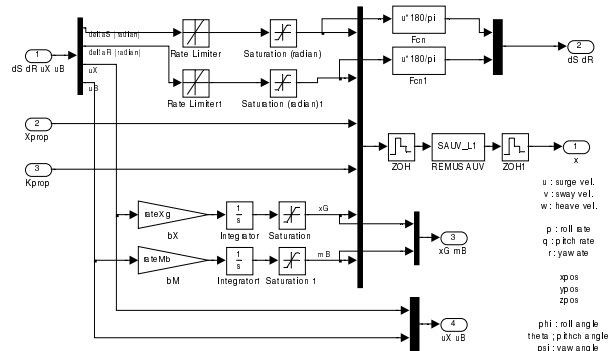


Fig. 5. Implementation of U_Glider(ZOH) block.

Table 2. AUV Parameters used for simulation (unit: MKS).

$m_h = 30.4791$	$x_b = 0$	$I_{xx} = 0.1770$
$\bar{m} = 1$	$y_b = 0$	$I_{yy} = 3.4500$
$m = 32.3140$	$z_b = 0$	$I_{zz} = 3.4500$
$g = 9.8100$	$x_g = 0$	
	$y_g = 0$	
	$z_g = 0.0200$	
$X_{\dot{u}} = -0.9300$	$Y_{v v} = -1310$	$Z_{w w} = -131$
$Z_{\dot{w}} = -35.5000$	$Y_{r r} = 0.6320$	$Z_{q q} = -0.6320$
$Z_{\dot{q}} = -1.9300$	$Y_{uvl} = -18.9600$	$Z_{uwl} = -18.9600$
$Y_{\dot{v}} = -35.5000$	$Y_{uu\delta r} = 9.6400$	$Z_{uu\delta s} = -9.6400$
$Y_{\dot{r}} = 1.9300$	$Y_{uvf} = -9.6400$	$Z_{uvf} = -9.6400$
$X_{u u} = -3.9000$	$Y_{urf} = 6.1500$	$Z_{uqa} = 0.9300$
		$Z_{uqf} = -6.1500$
$K_p = -0.0704$	$M_{\dot{w}} = -1.9300$	$N_{\dot{v}} = 1.9300$
$K_{r q} = -0.1300$	$M_{\dot{q}} = -4.8800$	$N_{\dot{r}} = -4.8800$
	$M_{w w} = 3.1800$	$N_{v v} = -3.1800$
	$M_{q q} = -188$	$N_{r r} = -94$
	$M_{uwl} = -4.4200$	$N_{uwl} = 4.4500$
	$M_{uu\delta s} = -6.1500$	$N_{uu\delta r} = -6.1500$
	$M_{uvf} = -6.1500$	$N_{uvf} = 6.1500$
	$M_{uqf} = -3.9300$	$N_{urf} = -3.9300$

$$Q = \text{diag}(10,10,10,0.001,10,100,100),$$

$$R = \text{diag}(1000,1000).$$

For the case when $\xi_d = \pm 30^\circ$ from Table 1, feedback gains K in (31) are obtained;

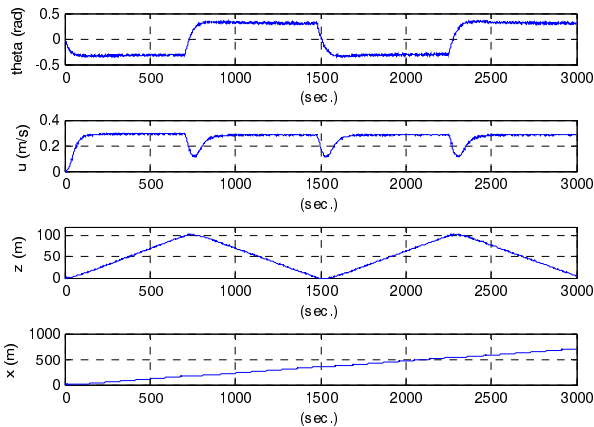
$$K = \begin{bmatrix} 0.1275 & -0.0477 & -0.0021 & -0.0009 \\ 0.0685 & -0.0195 & -0.0021 & -0.0004 \\ 0.0253 & 18.2924 & 0.4136 \\ 0.0110 & 6.9030 & 0.6220 \end{bmatrix}$$

for downward flight and

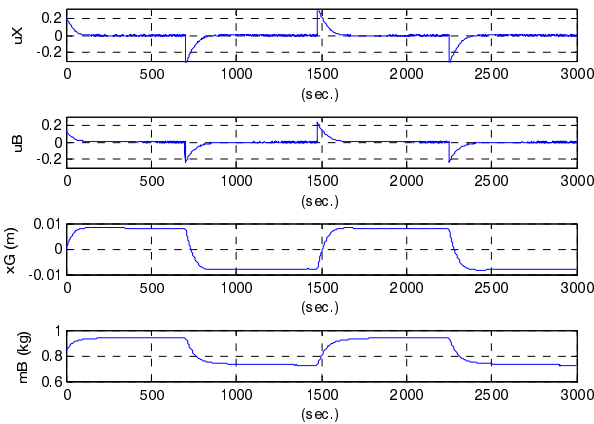
$$K = \begin{bmatrix} -0.1278 & -0.0481 & -0.0074 & -0.0009 \\ -0.0683 & -0.0196 & -0.0049 & -0.0004 \\ 0.0253 & 18.2666 & 0.4104 \\ 0.0109 & 6.8504 & 0.6195 \end{bmatrix}$$

for upward flight.

The simulation started from the surface and the target depth was given as a sequence of (100 m, 0 m, 100 m, 0 m, ...). When the AUV reached within 1 m from the target depth, the controller changed feedback gain according to the upward or downward flight and the target depth was changed to the next one.



(a) Attitude, surge, and position of the robot.



(b) Control efforts and the changes in center of gravity and buoyancy mass.

Fig. 6. Simulation results when $\xi_d = \pm 30^\circ$.

The simulation demonstrated the AUV moving forward by the controlled vertical zigzag movement as shown in Fig. 6(a). It showed that the AUV moved forward about 800 m by two laps of upward and downward movements, when the values of θ , u were controlled to the values θ_d , u_d in Table. 1. In Fig. 6(b), control efforts u_x , u_b were mainly occurred when the flight direction was to be changed which is common to the underwater glider, because it means low energy consumption. It also showed that x_g , m_b were well controlled to the values x_{gd} , m_{bd} by the proposed LQR controller.

6. CONCLUSION

The conventional autonomous underwater vehicle uses one or a few thrusters to go forward and consumes much energy, which limits the operation range of the vehicle. Conversely, the underwater glider uses the changes in the center of gravity and the net buoyancy to go forward, consuming much less energy. To combine the good aspects of both, we assumed an autonomous underwater vehicle with a moving battery and a buoyancy bag in its hull to add a gliding capability to the conventional autonomous underwater vehicle.

The stable gliding condition for the underwater vehicle was derived not by using the typical glider model but by the model of the conventional autonomous underwater vehicle. By using the resultant values as the set points, an LQR controller was designed and its effectiveness was demonstrated.

Proposed modeling method is beneficial because the parameters of the autonomous underwater vehicle are available for both autonomous underwater vehicle operation and underwater glider operation. Before this research, the optimal condition for the gliding operation was investigated only by the underwater glider model, because the set of the parameters was totally different from that of the autonomous underwater vehicle.

Future research is necessary to implement the proposed underwater vehicle and to verify the experimental results based on the theoretical research.

REFERENCES

- [1] T. Presto, *Verification of a Six-degree of Freedom Simulation Model for the REMUS Autonomous Underwater Vehicle*, M.S. thesis, Applied Ocean Science and Engineering, MIT & WHOI, 2001.
- [2] D. R. Yoerger, M. Jakuba, A. M. Bradley, and B. Bingham, "Techniques for deep sea near bottom survey using an autonomous underwater vehicle," *The International Journal of Robotics Research*, vol. 26, no. 1, pp. 41-54, 2007.
- [3] P. E. Hagen, N. Størkersen, B.-E. Marthinsen, G. Sten, and K. Vestgård, "Rapid environmental assessment with autonomous underwater vehicles-Examples from HUGIN operations," *Journal of Marine Systems*, vol. 69, no. 1-2, pp. 137-145, 2008.
- [4] B.-H. Jun, J.-Y. Park, F.-Y. Lee, P.-M. Lee, K. Kim, Y.-K. Lim, and J.-H. Oh, "Development of the

- AUV 'ISiMI' and a free running test in an ocean engineering basin," *Ocean Engineering*, vol. 36, no. 1, pp. 2-14, 2009.
- [5] L. A. Cooney, *Dynamic Response and Maneuvering Strategies of a Hybrid Autonomous Underwater Vehicle in Hovering*, M.S. thesis, Mechanical engineering, MIT, 2009.
- [6] A. Alvarez, "Redesigning the SLOCUM glider for torpedo tube launching," *IEEE Journal of Oceanic Engineering*, vol. 35, no. 24, pp. 984-991, 2010.
- [7] D. C. Webb, P. J. Simonetti, and C. P. Jones, "SLOCUM: an underwater glider propelled by environmental energy," *IEEE Journal of Oceanic Engineering*, vol. 26, no. 4, pp. 447-452, 2001.
- [8] C. C. Eriksen, T. J. Osse, R. D. Light, T. Wen, T. W. Lehman, P. L. Sabin, J. W. Ballard, and A. M. Chiodi, "Seaglider: a long-range autonomous underwater vehicle for oceanographic research," *IEEE Journal of Oceanic Engineering*, vol. 26, no. 4, pp. 424-436, 2001.
- [9] J. Sherman, R. E. Davis, W. B. Owens, and J. Valdes, "The autonomous underwater glider 'Spray'," *IEEE Journal of Oceanic Engineering*, vol. 26, no. 4, pp. 437-446, 2001.
- [10] W. P. Barker, *An Analysis of Undersea Glider Architectures and an Assessment of Undersea Glider into Undersea Applications*, M.S. thesis, Dept. Systems Eng., Naval Postgraduate School, 2012.
- [11] A. Alvarez, A. Caffaz, A. Caiti, G. Casalino, L. Gualdesi, A. Turetta, and R. Viviani, "Fòlaga: A low-cost autonomous underwater vehicle combining glider and AUV capabilities," *Ocean Engineering*, vol. 36, no. 1, pp. 24-38, 2009.
- [12] ASCA-ALCEN, SeaExplorer - autonomous underwater vehicle gliders, <http://www.underwater-gps.com/images/dynproduits/g48.pdf>, March 28, 2014.
- [13] J. Imlach and R. Mahr "Modification of a military grade glider for coastal scientific applications," *Proc. of IEEE Oceans*, pp. 1-6, 2012.
- [14] S.-X. Wang, X.-J. Sun, Y.-H. Wang, J.-G. Wu, and X.-M. Wang, "Dynamic modeling and motion simulation for a winged hybrid-driven underwater glider," *China Ocean Engineering*, vol. 25, no. 1, pp. 97-112, 2011.
- [15] J. G. Bellingham, Y. Zhang, J. E. Kerwin, J. Erikson, B. Hobson, B. Kieft, M. Godin, R. McEwen, T. Hoover, J. Paul, A. Hamilton, J. Franklin, and A. Banka, "Efficient propulsion for the Tethys long-range autonomous underwater vehicle," *Proc. of IEEE/OES Autonomous Underwater Vehicles (AUV)*, pp. 1-7, 2010.
- [16] R. Cristi, F. A. Papoulias, and A. J. Healey, "Adaptive sliding mode control of autonomous underwater vehicles in the dive plane," *IEEE Journal of Oceanic Engineering*, vol. 15, no. 3, pp. 152-160, 1990.
- [17] A. J. Healey and D. Lienard, "Multivariable sliding-mode control for autonomous diving and steering of unmanned underwater vehicles," *IEEE Journal of Oceanic Engineering*, vol. 18, no. 3, pp. 327-339, 1993.
- [18] B. Jalving, "The NDRE-AUV flight control system," *IEEE Journal of Oceanic Engineering*, vol. 19, no. 4, pp. 497-501, 1994.
- [19] G. Antonelli, S. Chiaverini, N. Sarkar, and M. West, "Adaptive control of an autonomous underwater vehicle: experimental results on ODIN," *IEEE Trans. Control Systems Technology*, vol. 9, no. 5, pp. 756-765, 2001.
- [20] J.-S. Wang and C. S. G. Lee, "Self-adaptive recurrent neuro-fuzzy control of an autonomous underwater vehicle," *IEEE Trans. Robotics and Automation*, vol. 19, no. 2, pp. 283-295, 2003.
- [21] J. G. Graver, *Underwater Gliders: Dynamics, Control and Design*, Ph.D. thesis, Dept. mechanical and aerospace Eng., Princeton University, 2005.
- [22] N. E. Leonard and J. G. Graver, "Model-based feedback control of autonomous underwater gliders," *IEEE Journal of Oceanic Engineering*, vol. 26, no. 4, pp. 633-644, 2001.
- [23] N. A. A. Hussain, M. R. Arshad, and R. Mohd-Mokhtar, "Underwater glider modelling and analysis for net buoyancy, depth and pitch angle control," *Ocean Engineering*, vol. 38, no. 16, pp. 1782-1791, 2011.
- [24] N. Mahmoudian, J. Geisbert, and C. Woolsey, "Approximate analytical turning conditions for underwater gliders: Implications for motion control and path planning," *IEEE Journal of Oceanic Engineering*, vol. 35, no. 1, pp. 131-143, 2010.
- [25] M. Nakamura, K. Asakawa, T. Hyakudome, S. Kishima, H. Matsuoka, and T. Minami, "Hydrodynamic coefficients and motion simulations of underwater glider for virtual mooring," *IEEE Journal of Oceanic Engineering*, vol. 38, no. 3, pp. 581-597, 2013.
- [26] S. Zhang, J. Yu, A. Zhang, and F. Zhang, "Spiraling motion of underwater gliders: modeling, analysis, and experimental results," *Ocean Engineering*, vol. 60, pp. 1-13, 2013.
- [27] J. Yu, F. Zhang, A. Zhang, W. Jin, and Y. Tian, "Motion parameter optimization and sensor scheduling for the sea-wing underwater glider," *IEEE Journal of Oceanic Engineering*, vol. 38, no. 2, pp. 243-254, 2013.
- [28] T. I. Fossen, *Guidance and Control of Ocean Vehicles*, John Wiley & Sons, Ltd., 1994.
- [29] T. I. Fossen, *Handbook of Marine Craft Hydrodynamics and Motion Control*, John Wiley & Sons, Ltd., 2011.



Moon G. Joo received his B.S. degree in Electronics And Electric Engineering, an M.S. in Computer and Communications Engineering, and a Ph.D. in Electrical and Computer Engineering from Pohang University of Science and Technology, Pohang, Korea, in 1992, 1994, and 2001, respectively. Dr. Joo was a senior researcher at Research Institute of Indus-

trial Science and Technology, Pohang, Korea from 1996 to 2003. Since 2003, he has been a professor of Pukyong National University, Busan, Korea. Recently, he has been with the Department of Electrical Engineering and Computer Science, University of Central Florida, FL, for his sabbatical leave. His research interests include factory automation, intelligent control, and underwater vehicles.



Zhihua Qu received his Ph.D. degree in Electrical Engineering from the Georgia Institute of Technology, Atlanta, in 1990. Since then, he has been with the University of Central Florida, Orlando, where he is currently SAIC Endowed Professor and Chair of Electrical and Computer Engineering. He has published a number of papers in these areas and is the author

of three books, *Robust Control of Nonlinear Uncertain Systems* (Wiley Interscience, 1998), *Robust Tracking Control of Robotic Manipulators* (IEEE Press, 1996), and *Cooperative Control of Dynamical Systems* (Springer-Verlag, 2009). He served or has been serving on the Board of Governors, IEEE CSS and as an Associate Editor for *Automatica*, *IEEE ACCESS*, *IEEE Transactions on Automatic Control*, and the *International Journal of Robotics and Automation*. His main research interests are nonlinear and networked systems, cooperative and robust controls, robotics and autonomous vehicle systems, and energy systems.